Published in final edited form as:
Nanoscale. 2012 November 21; 4(22): . doi:10.1039/c2nr32055j.

A Versatile Method for Generating Semiconducting Polymer Dot Nanocomposites

Wei Sun, **Sarah Hayden**, **Yuhui Jin**[a], **Yu Rong**, **Jiangbo Yu**, **Fangmao Ye**, **Yang-Hsiang Chan**[b], **Max Zeigler**, **Changfeng Wu**[c], and **Daniel T. Chiu**
Department of Chemistry, University of Washington, Seattle, Washington 98195, USA. chiu@chem.washington.edu; FAX: 206 685 8665; TEL: 206 543 1655.

Abstract

This paper describes a method, based on co-precipitation, for generating small semiconducting polymer dot (Pdot) nanocomposites, which contain either gold or iron oxide nanoparticles within the Pdot matrix. We demonstrate the utility of Pdot-Au nanoparticles (Au-NP-Pdots) in dual-modality imaging in which co-localization of fluorescence from Pdot and scattering from Au was used to identify Au-NP-Pdot probes for downstream single-particle tracking and cellular imaging. We also demonstrate the potential of employing Pdot-FeO_x nanoparticles (FeO_x-NP-Pdots) for both sample preparation, where cells tagged with FeO_x-NP-Pdots were isolated using an external magnet, and cellular imaging and detection, owing to the intense fluorescence from Pdots. The method we present here should be generalizable to the formation of other Pdot nanocomposites for creating the next generation of multi-functional Pdot probes.

Introduction

Semiconducting polymer dots (Pdots) have recently emerged as a new type of fluorescent nanoprobes that hold great promise. [1–9] Compared to small fluorescent dyes and quantum dots, Pdots possess high brightness, fast emission rates, and good photo-stability.[1, 6] The size of Pdots also can be tuned from several to tens of nanometers without affecting their emission spectra.[1] In addition to demonstrating the usefulness of Pdots for cellular labelling in cell-culture studies[3, 6, 10], we have also shown that their excellent optical properties lend themselves well to *in vivo* imaging applications.[7]

The motivation to further broaden the applications of Pdots has prompted us and others to prepare Pdot-based hybrid nanoparticles.[11–14] Because the properties of different nanomaterials can be integrated to ideally complement each other, Pdot-based hybrid nanoparticles can provide additional functionalities that are not available to Pdots alone. For example, we prepared hybrid nanoparticles with quantum dots (Qdots) embedded in Pdots (Pdot-Qdot) by covalently linking semiconducting polymers functionalized with amine groups to the surface of Qdots.[11] The hybrids showed narrow-band and near-IR fluorescence emission with high brightness. Besides Qdots, many other inorganic nanoparticles exist and can be used to prepare Pdot based hybrid nanoparticles for a wide range of applications. For

Correspondence to: Daniel T. Chiu.

[a]Current address: Corning Inc., Painted Post, NY, 14831 USA.
[b]Current address: Department of Chemistry, National Sun Yat-Sen University, Kaohsiung, 80424 Taiwan.
[c]Current address: Jilin University, Changchun, Jilin, 130012, P. R. China.

[†]Electronic Supplementary Information (ESI) available: Pdot synthesis, cell culture, cell immuno-labeling and imaging instrumentation. See DOI: 10.1039/b000000x/

example, gold nanoparticles (Au NPs) have been used as contrast agents for long-term observation and single-particle tracking in dark-field microscopy because Au NPs do not photobleach.[15] But in dark-field microscopy, it is difficult to distinguish Au NPs from other intracellular micro- and nano-features that also strongly scatter light and thus give rise to signals similar to Au NPs. This problem can be overcome by embedding Au NPs within Pdots to endow the hybrid nanoparticles dual-modality imaging capability. In this way, Au-NP-Pdots can be differentiated easily from other cellular features because only they can generate both strong dark-field and fluorescence signals. Here, fluorescence is used to help identify true Au-NP-Pdot probes and dark-field is then used to carry out long-term imaging to take advantage of the optical stability of Au nanoparticles.

To prepare Pdots, there are two main approaches. One is based on miniemulsion and the other is based on nanoprecipitation.[5, 16] In the miniemulsion approach, amphiphilic surfactant molecules are used to form water-miscible micelles that contain the hydrophobic semiconducting polymers. Recently, this strategy was used to prepare nanoparticles that contained both semiconducting polymers and iron oxide or gold nanoparticles.[12–14] However, these hybrids contained a fairly small percentage of fluorescent semiconducting polymers (only ~ 1.2% – 8% of the host matrix was semiconducting polymer) and they were also quite large, ranging from ~120 nm[12] to around ~180 nm[13]. Smaller nanoparticles are often more desirable because they usually possess better cellular labelling and biodistribution properties. In comparison to the miniemulsion method, Pdots prepared by nanoprecipitation are usually smaller and can be easily conjugated to biomolecules, such as streptavidin, by covalent bonding.[3, 6] Here, we describe a simple and versatile method for generating Pdot nanocomposites using nanoprecipitation, and demonstrate this method by creating Pdot hybrids that have either embedded gold nanoparticles (Au-NP-Pdots) or iron oxide nanoparticles (FeO_x-NP-Pdots). The hybrid nanoparticles are smaller than those synthesized by the miniemulsion method, and the number of embedded inorganic nanoparticles can be reduced to a single one. The new hybrid nanoparticles can also be easily modified with biomolecules on their surface and used for specific cellular labelling and targeting applications.

Results and discussion

Previous reports have described how nanoprecipitation can be used to dope hydrophobic organic dyes into Pdots by simply mixing the dye molecules with semiconducting polymers in tetrahydrofuran (THF) prior to injection into water.[17–19] Co-precipitation of the hydrophobic dye molecules with the semiconducting polymers during nanoprecipitation resulted in doped Pdots. The collapsed hydrophobic chains of the polymers served as a good host matrix for encapsulating the hydrophobic dyes. Inspired by this finding, we generated Au and FeO_x nanoparticles embedded Pdots. The key step was to passivate the surface of inorganic nanoparticles with a layer of hydrophobic molecules. Once the surface of Au or FeO_x nanoparticles became hydrophobic, they could be dispersed homogeneously in THF with the semiconducting polymers. As with the hydrophobic dyes, the Au or FeOx nanoparticles mixed with the semiconducting polymers in THF then formed Au-NP-Pdots or FeO_x-NP-Pdots during nanoprecipitation. Furthermore, by controlling the relative amounts of inorganic nanoparticles and semiconducting polymers as well as by taking advantage of the facile density-based separation of Au-NP-Pdots or FeO_x-NP-Pdots from empty Pdots, we generated hybrid Pdots that had consisted of only one Au or FeO_x nanoparticle.

Au nanoparticles were first synthesized in aqueous solution (see figure S1), and then modified to become hydrophobic on the surface via phase-transfer into toluene, assisted by thiol-terminated polystyrene. After phase-transfer, the upper toluene solution was centrifuged to collect the hydrophobic Au nanoparticles. The nanoparticle pellet was re-

dispersed in THF together with the hydrophobic semiconducting polymer. This THF solution was then injected into pure water under sonication to produce the final Au-NP-Pdot hybrids (Scheme 1). For the FeO_x nanoparticles that we purchased, they already had a hydrophobic surface and were well dispersed in toluene. Therefore, we directly centrifuged the FeO_x nanoparticles and redispersed them in THF with the semiconducting polymers.

To ensure that all the Au and FeO_x nanoparticles present in solution were encapsulated within Pdots, the concentration of the semiconducting polymers in solution was generally kept higher than that of inorganic nanoparticles. As expected, there were many empty Pdots. However, it was straightforward to isolate the Pdots with Au or FeO_x nanoparticles from empty ones because the Au-NP-Pdots and FeO_x-NP-Pdots have a much higher density than the empty Pdots. Figure 1A shows the purification procedure, in which we used a sucrose step gradient. The heavier Au-NP-Pdots penetrated the sucrose layer and settled at the bottom of the centrifuge tube, while the lighter empty Pdots stayed above the sucrose layer. Figure 1A also shows transmission electron microscopy (TEM) images of Pdots retrieved from the solution above the sucrose layer and those at the bottom of the centrifuge tube. In the TEM images, we did not see any empty Pdots in the Pellet, or any Au-NP-Pdots in the top fraction. This result indicates the successful purification of Au-NP-Pdots from empty Pdots with nearly 100% yield. For this experiment, we used a high concentration of Au nanoparticles, which resulted in large Pdots (64 nm in diameter) that contained multiple Au nanoparticles.

The size of the Au-NP-Pdots could be further reduced when the number of embedded Au nanoparticles decreased. For example, when the concentration of initially added Au nanoparticles was sufficiently low, the occupancy of Au nanoparticles per Pdot decreased. Pdots containing only a single Au nanoparticle were generated (Figure 1B). We measured the average size of singly occupied Au-NP-Pdots to be 28 nm. This strategy for generating Pdots with single encapsulated nanoparticles also worked well for FeO_x-NP-Pdots (Figure 1C).

We next characterized the optical properties of the Au-NP-Pdot and FeO_x-NP-Pdot hybrids. Au-NP-Pdots had a new peak at 525 nm in the absorption spectrum that was distinct from the peak obtained from pure PFO Pdots (figure 2A). This new peak was from the characteristic Localized Surface Plasmon Resonance (LSPR) of Au nanoparticles. Compared to bare Au nanoparticles dispersed in water, the LSPR peak of Au-NP-Pdots was slightly red-shifted. This red shift was caused by the close proximity between Au nanoparticles and the change in the local environment around the Au nanoparticles because the Pdot matrix has a higher refractive index than water. The emission spectra of Au-NP-Pdots and pure PFO Pdots were also measured and found to be similar or identical. As shown in figure 2B, the absorption peak for FeO_x-NP-Pdots was a little broadened because of the wide band absorption of FeO_x NPs; the shape of fluorescence emission spectrum of the semiconducting polymer was not affected by the FeO_x NPs.

The nanoparticle within the Pdot has the potential to quench the Pdot's fluorescence.[20] To determine the extent of this potential issue, we measured the quantum yield (QY) values of the various Pdots and Pdot nanocomposites. The QY value for pure PFO Pdots was 37%; for Au-NP-PFO Pdots with multiple Au NPs, it was 7%. When the number of Au nanoparticles per Pdot decreased to 1, the QY of Au-NP-Pdot increased to 18%. Given the fact that each Pdot can be 30 times brighter than a quantum dot,[6] this 2 to 5 fold decrease in QY is manageable. It should also be noted that the fluorophore density of the hybrid Pdot nanoparticles prepared with our method is significantly higher than that of hybrid nanoparticles prepared with the miniemulsion method. For example, in our Pdot-nanoparticle hybrid, ~90 % (10 parts semiconducting polymer, 1 part PS-PEG-COOH) of

the host matrix is fluorescent semiconducting polymer; only ~ 1.2% – 8% of the host matrix was fluorescent semiconducting polymer in the reported hybrid nanoparticles.[12, 14] Therefore, the Pdot nanocomposites prepared using the method described here overall retained much of their desirable optical characteristics.

To test whether or not Au-NP-Pdots could serve as dualmodality imaging probes for both dark-field and fluorescence microscopy, we imaged them using a fluorescence microscope equipped with dark-field optics. Individual Au-NP-Pdots were imaged with excellent signal-to-noise ratio in both dark-field and fluorescence mode (figure 3A). The positions of all the Au-NP-Pdots in the two images were correlated. We also imaged the Au-NP-Pdots inside mammalian cells, which represent a more complex environment (figure 3B). In dark-field mode, many cellular organelles also strongly scattered light, which made it difficult to differentiate them from Au nanoparticles. When switched into fluorescence mode, the number of bright spots decreased (figure 3B). Each bright spot in fluorescence image had a corresponding bright spot in the dark-field image. Considering that only Au-NP-Pdots can generate both strong fluorescence and scattering signals, we were able to pinpoint the bright spots that appeared in the dark-field image to the six spots (pointed to by arrows) that were from Au-NP-Pdots. Because conjugated polymers do not corrode or damage Au nanoparticles under the illumination light in normal dark field microscopy, Au nanoparticles' dark-field scattering photo-stability should not change. Because Au nanoparticles do not photobleach, they were suitable for long-term particle tracking and imaging in dark-field mode; the fluorescence from the Pdots helped to distinguish these Pdot nanocomposites from other nanoscale cellular features that scattered light.

For FeO_x-NP-Pdots, we tested their potential application in both bioimaging and sample preparation. We successfully prepared FeO_x-NP-Pdots containing magnetic nanoparticles of various sizes (10 nm, 20 nm and 40 nm) (see figure S2). We showed that these FeO_x-NP-Pdots were attracted to and concentrated by a magnet; these hybrid FeO_x-NP-Pdots emitted strong fluorescence when excited by UV light (figure 4A). During FeO_x-NP-Pdot preparation, the high molecular weight polymer PS-PEG-COOH was blended into the Pdot nanocomposites. The carboxylic acid groups on the Pdots' surface enabled facile bioconjugation with streptavidin through a simple EDC reaction (figure 4B). We then labeled the MCF-7 cancer cell line with streptavidin-conjugated FeO_x-NP-Pdots and a biotinylated primary antibody against EpCAM, a cell-surface protein commonly used to isolate circulating tumor cells. The FeO_x-NP-Pdots labeled cells could be manipulated and enriched using a permanent magnet (figure 4C). In figure 4C, it can be seen that the majority of labelled cells were successfully attracted to the magnet. Given that stronger magnet and magnetic nanoparticles can be used, the cell separation efficiency may be further improved if necessary. To further confirm that cells concentrated by the magnet had FeO_x-NP-Pdots, the isolated cells were imaged by fluorescence microscopy, which confirmed the presence of FeO_x-NP-Pdots on the cell surface (figure 4C). In this way, FeO_x-NP-Pdots can be used for cell enrichment and isolation, similar to the use of iron-oxide nanoparticles for immuno-magnetic isolation, as well as for cellular imaging and detection by taking advantage of the strong fluorescence signal from Pdots.

Conclusions

In summary, we successfully developed a nanoprecipitation procedure to generate Pdot nanocomposites that contained either gold or iron oxide nanoparticles. The Pdot nanocomposites prepared by this method exhibited smaller sizes in comparison to hybrid Pdot nanoparticles prepared by the miniemulsion method. By controlling the ratio of nanoparticles and polymers during preparation as well as taking advantage of the easy separation between empty Pdots from those with encapsulated nanoparticles, we created

Pdots that contained a single encapsulated nanoparticle. The Pdot nanocomposite prepared by our method retained the high brightness of Pdots and provided additional functionality, such as enhanced bioimaging capability and sample preparation. We anticipate this method can be generalized for the preparation of a wide range of Pdot nanocomposites with different functionalities.

Supplementary Material

Refer to Web version on PubMed Central for supplementary material.

Acknowledgments

D.T.C. acknowledges support for his research from the NIH (R21CA147831) and NSF (CHE-0924320).

Notes and references

1. Wu C, Bull B, Szymanski C, Christensen K, McNeill J. ACS Nano. 2008; 2:2415–2423. [PubMed: 19206410]
2. Wu CF, Szymanski C, Cain Z, McNeill J. J. Am. Chem. Soc. 2007; 129:12904–12905. [PubMed: 17918941]
3. Wu CF, Jin YH, Schneider T, Burnham DR, Smith PB, Chiu DT. Angew. Chem.-Int. Edit. 2010; 49:9436–9440.
4. Tian ZY, Yu JB, Wu CF, Szymanski C, McNeill J. Nanoscale. 2010; 2:1999–2011. [PubMed: 20697652]
5. Pecher J, Mecking S. Chem. Rev. 2010; 110:6260–6279. [PubMed: 20684570]
6. Wu CF, Schneider T, Zeigler M, Yu JB, Schiro PG, Burnham DR, McNeill JD, Chiu DT. J. Am. Chem. Soc. 2010; 132:15410–15417. [PubMed: 20929226]
7. Wu C, Hansen SJ, Hou Q, Yu J, Zeigler M, Jin Y, Burnham DR, McNeill JD, Olson JM, Chiu DT. Angewandte Chemie International Edition. 2011; 50:3430–3434.
8. Ye FM, Wu CF, Jin YH, Chan YH, Zhang XJ, Chiu DT. J. Am. Chem. Soc. 2011; 133:8146–8149. [PubMed: 21548583]
9. Wu CF, Szymanski C, McNeill J. Langmuir. 2006; 22:2956–2960. [PubMed: 16548540]
10. Ye F, Wu C, Jin Y, Wang Y-H, Chan M, Yu J, Sun W, Hayden S, Chiu DT. Chem. Commun. 2012:1778–1780.
11. Chan Y-H, Ye F, Gallina ME, Zhang X, Jin Y, Wu IC, Chiu DT. J. Am. Chem. Soc. 2012; 134:7309–7312. [PubMed: 22515545]
12. Geng J, Li K-Y, Pu K, Ding D, Liu B. Small. 2012; 8:2421–2419. [PubMed: 22544732]
13. Li K, Ding D, Huo K-Y, Pu D, Thao NNP, Hu Y, Li Z, Liu B. Adv. Funct. Mater. 2012; 22:3107–3115.
14. Howes P, Green M, Bowers A, Parker D, Varma G, Kallumadil M, Hughes M, Warley A, Brain A, Botnar R. J. Am. Chem. Soc. 2010; 132:9833–9842. [PubMed: 20572665]
15. Wang GF, Stender AS, Sun W, Fang N. Analyst. 2010; 135:215–221. [PubMed: 20098755]
16. Tuncel D, Demir HV. Nanoscale. 2010; 2:484–494. [PubMed: 20644748]
17. Wu CF, Zheng YL, Szymanski C, McNeill J. J. Phys. Chem. C. 2008; 112:1772–1781.
18. Jin YH, Ye FM, Zeigler M, Wu CF, Chiu DT. ACS Nano. 2011; 5:1468–1475. [PubMed: 21280613]
19. Wu CF, Bull B, Christensen K, McNeill J. Angew. Chem.-Int. Edit. 2009; 48:2741–2745.
20. Jain PK, Lee KS, El-Sayed IH, El-Sayed MA. J. Phys. Chem. B. 2006; 110:7238–7248. [PubMed: 16599493]

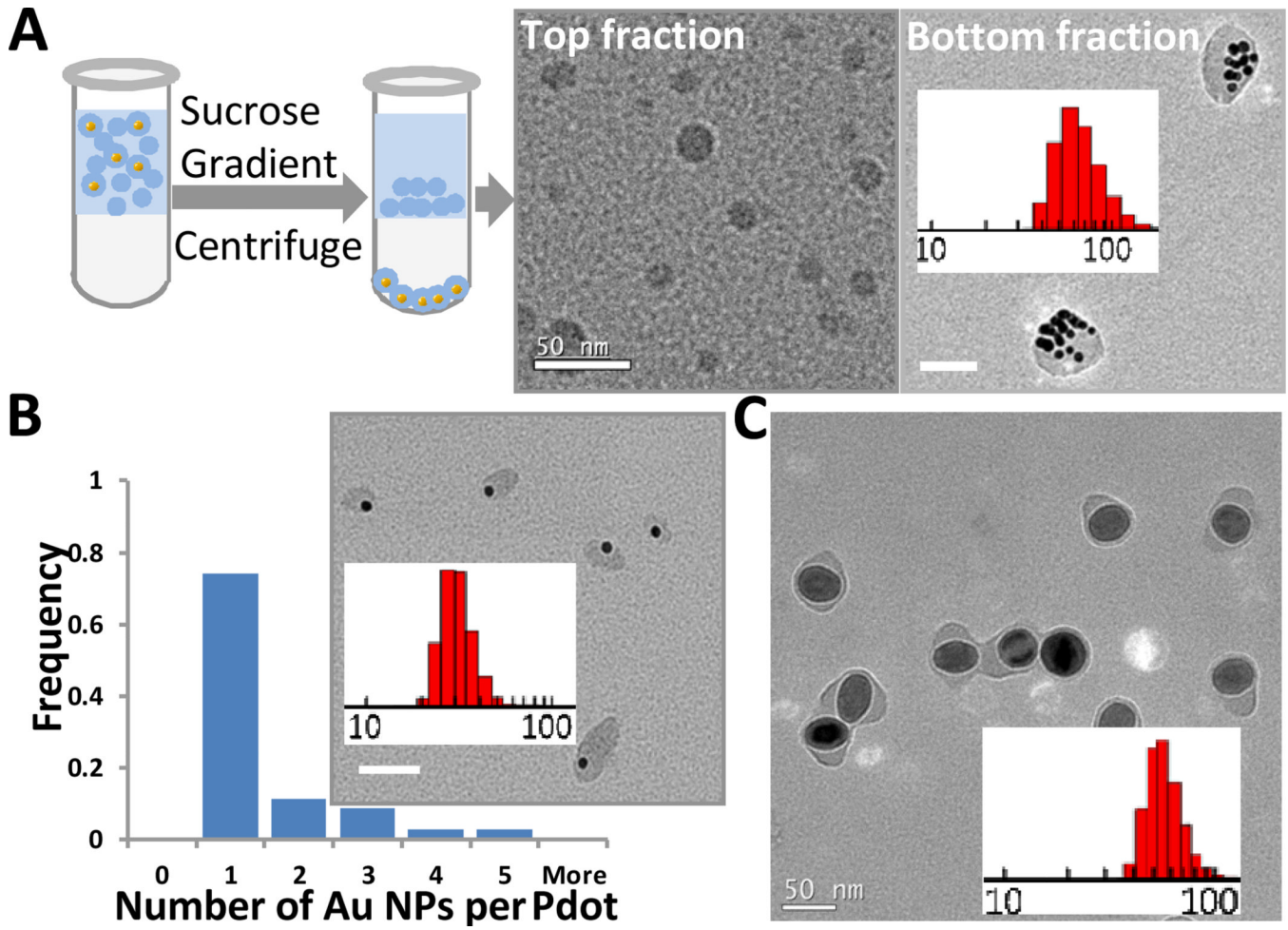

Fig. 1.

Separation of Pdots with gold or iron oxide nanoparticles from empty ones. **(A)** Schematic depicting the purification procedure using centrifugation with a step sucrose gradient. TEM images of empty Pdots retrieved from the fraction above the sucrose solution (left) and Au-NP-Pdots from the bottom fraction of the tube (right). The inset histogram shows the size distribution of Au-NP-Pdots. The average size was 65 nm. **(B)** TEM image of Pdots containing a single Au nanoparticle and a histogram showing the number of Au NPs in each Pdot. The average size was 28 nm. The inset histogram is the size distribution of Au-NP-Pdots. **(C)** TEM image of FeO_x-NP-Pdots. The average size was 52 nm. The FeO_x nanoparticles were 40 nm in diameter. The inset histogram is the size distribution of FeO_x-NP-Pdots. Scale bar represents 50 nm.

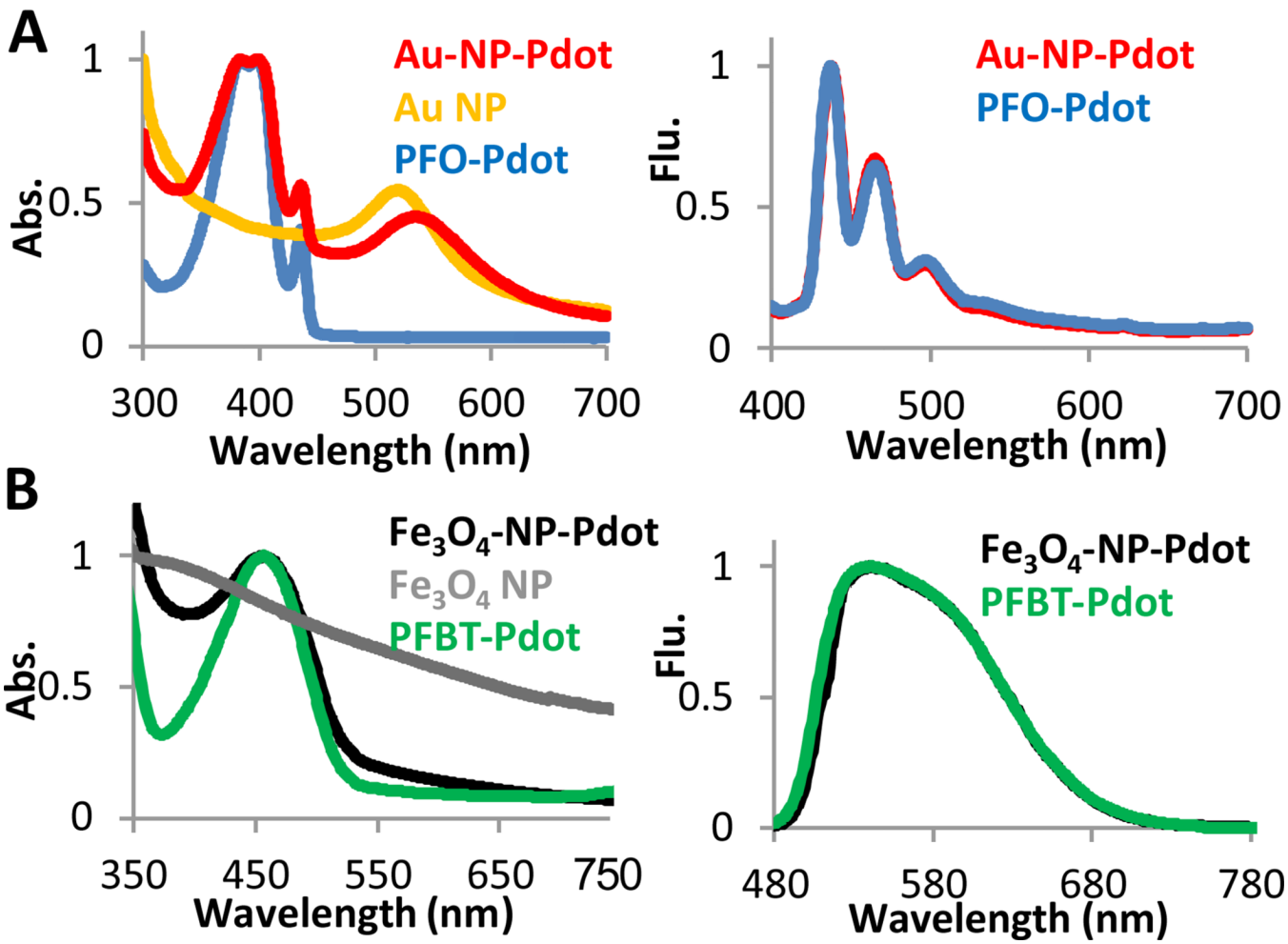

Fig. 2.

Optical characterization of hybrid Pdots. **(A)** The absorption (Abs.) and emission (Flu.) spectra of Au-NP-Pdots. The excitation wavelength was 380 nm, and the semiconducting polymer was PFO. **(B)** The absorption and emission spectra of FeO_x-NP-Pdots. The excitation wavelength was 457 nm, and the semiconducting polymer was PFBT.

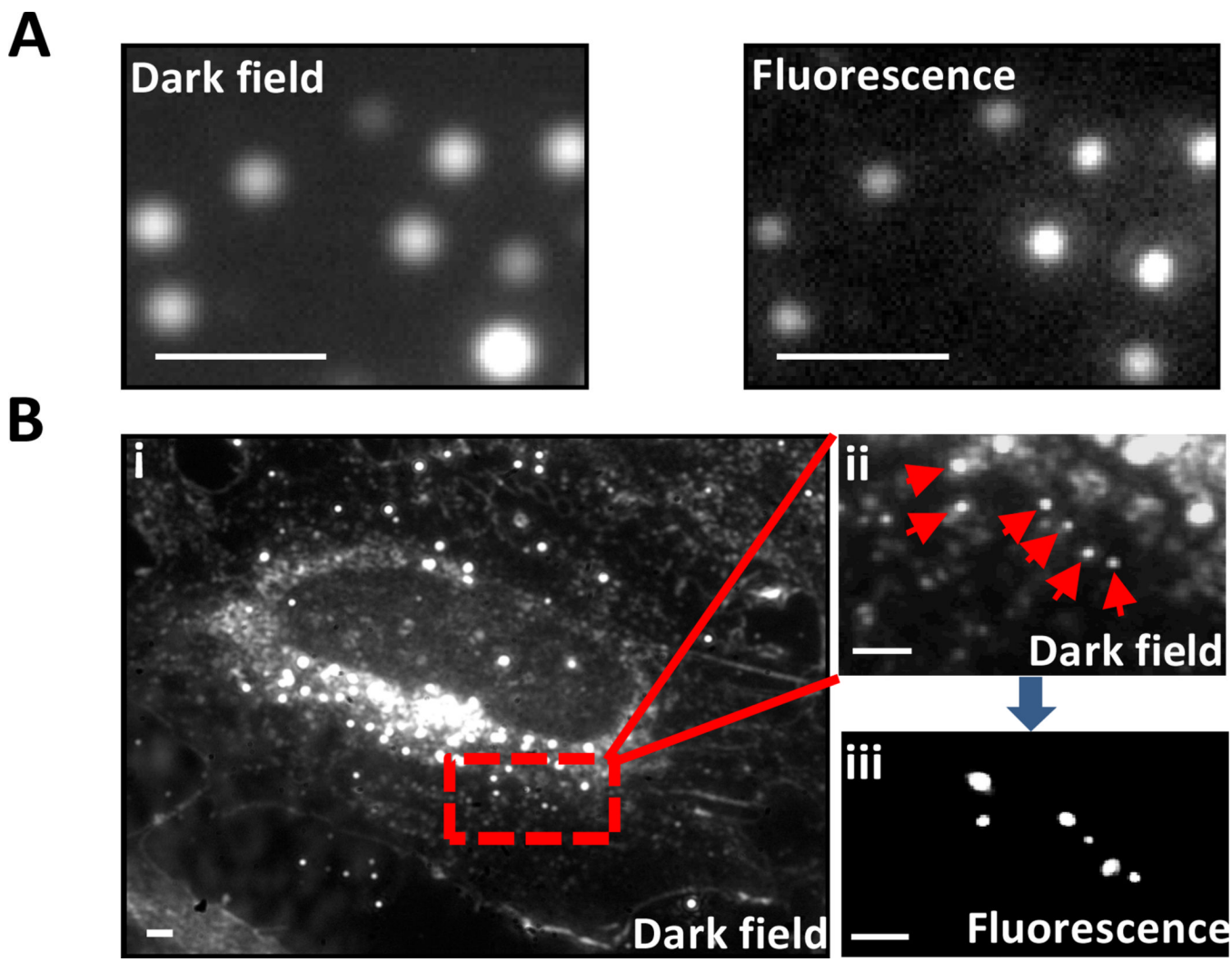

Fig. 3.

Dark field and fluorescence microscopy images of Au-NP-Pdots. **(A)** Dark-field (left) and fluorescence (right) images of Au-NP-Pdots immobilized on glass coverslip. **(B)** Dark-field and fluorescence images of Au-NP-Pdots inside cells. (i) Dark-field image of a whole cell; (ii) magnified image of the red rectangular area in (i); (iii) Corresponding fluorescence image of (ii). The Au-NP-Pdots were the same as those in figure 1A. Scale bar represents 1 μm.

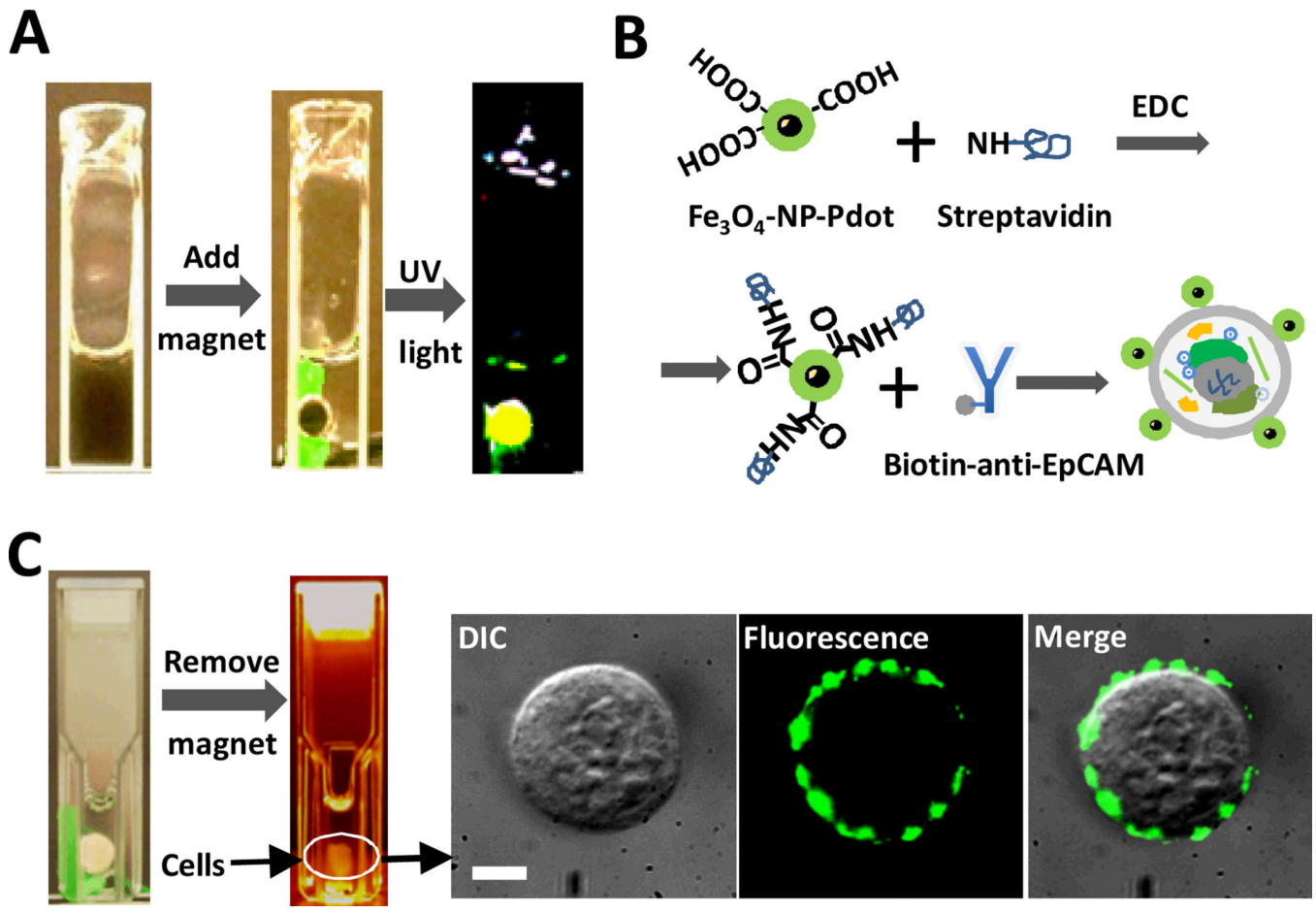

Fig. 4.

Immuno-magnetic isolation of cells labelled with FeO_x-NP-Pdots. **(A)** Manipulation of FeO_x-NP-Pdots dispersed in aqueous solution with a permanent magnet. **(B)** Schematic showing the bioconjugation of FeO_x-NP-Pdots to streptavidin for labelling the cell-surface protein, EpCAM. **(C)** Immuno-magnetic separation of cells labelled with FeO_x-NP-Pdots with a permanent magnet. Images to the right show an isolated cell. Scale bar represents 5 μm.

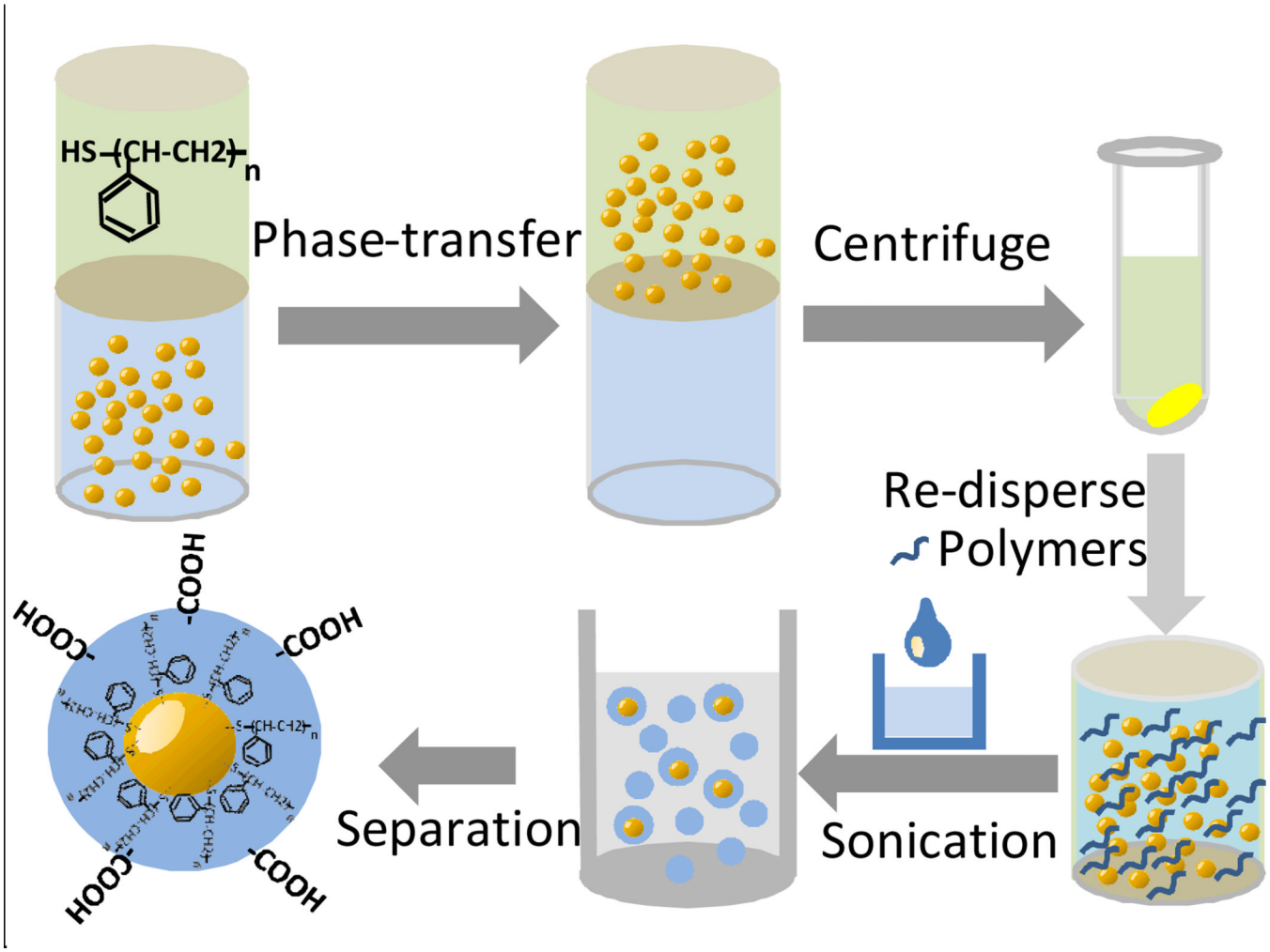

Scheme 1.
Schematic shows the procedure for generating Pdots, which have a single Au nanoparticle embedded in them.